A Preminary evaluation of the "simplified triangle" with Sentinel-3 images for mapping Surface Soil Moisture and Evaporative fluxes: results obtained in a Spanish savannah environment

George P. Petropoulos[1*] Sandric Ionut[2], Andrew Pavlides[1], Dionissios Hristopulos[1]

[1] School of Mineral Resources Engineering, Technical University of Crete, 73100, Crete, Greece
[2] Faculty of Geography, University of Bucharest, Bucharest, Romania

Correspondence: Email: petropoulos.george@gmail.com; gpetropoulos1@isc.tuc.gr

ABSTRACT

This study provides the first results from an initial exploration of the so-called "simplified triangle" for estimating evaporative fraction (EF) and surface soil moisture (SSM) from remotely sensed data of land surface temperature (Ts) and a vegetation index (VI) derived from ESA's Sentinel-3 satellite. The technique is implemented for 11 cloud free days of year 2018 in a typical savannah Meditteranean site located in Spain, which is part of the CarboEurope ground observational network. In overall, the preliminary results obtained demonstrated the potential of the technique in mapping both EF and SSM. A Root Mean Square Error (RMSE) of 0.063 and 0.048 vol vol^{-1} and correlation coefficient (R) of 0.777 and 0.439 for EF and SSM respectively was reported. Results are of considerable scientific and practical value in regards to the evaluation of the potential of the examined technique for deriving key biophysical parameters of the Earth's system.

KEYWORDS: Sentinel-3, SSM, EF, simplified triangle, Ts/VI domain, Fluxnet

1. Introduction

The land surface and atmosphere interact over a wide range of space and time scales, and include the interactions of numerous complex natural processes which influence the global climate system (Stoyanova and Georgiev, 2013; Petropoulos et al., 2016). Globally, climate change is facilitating large scale changes within the atmosphere, biosphere, geosphere and hydrosphere (Steinhauser et al. 2012). Quantification and management of such change have become an urgent and important research directions within numerous scientific disciplines (Coudert et al., 2007), as well as serving as essential information for politicians, policymakers and the wider global community (IPCC, 2009). In this context, accurate monitoring of parameters such as of evaporative fraction (defined as the ratio of instantaneous latent heat flux (LE) to net radiation (Rn)) and surface soil moisture (SSM) has a high priority within current EU frameworks, particularly communities in water-limited environments or areas which rely on rain-fed agriculture, such as the Mediterranean (Amriet al., 2014; European Commission, 2009).

Earth Observation (EO) allows today obtaining, at different spatial scales, temporally consistently coverage of both EF and SSM (Piles et al., 2016; Srivastava et al., 2019). Several EO-based approaches have been proposed for this purpose utilising spectral information acquired at different regions of the electromagnetic spectrum (see reviews by Petropoulos et al., 2015; 2018). Methods based in particular on the physical relationships between a satellite-derived surface temperature (Ts) and vegetation index (VI) have been very promising in that respect. Assuming conditions of full variability in fractional vegetation cover within the sensor's field of view, when plotted Ts and VI in a scatterplot a triangular (or trapezoidal) shape emeges. shape arises from Ts being less sensitive to water content at the surface in vegetated areas than in areas of exposed soil. Such a scatterplot encapsulates several key biophysical variables (e.g. see Gillies et al., 1997; Petropoulos et al., 2009; Maltese et al., 2015).

It has been demonstrated that the derivation of spatially distributed EF and/or SSM using the Ts/VI domain is feasible using a variety of approaches (see review by Petropoulos et al., 2009). Recently, Carlson & Petropoulos (2019) proposed a new technique for estimating both SSM and EF, which they named as "simplified triangle". Silva-Fuzzo et al. (2019) demonstrated its use coupled with a crop prediction and a climatological water balance model for predicting soybean yield using MODIS data. To our knowledge, implementation and verification of this new technique using ESA's Sentinels-3 has not been conducted in detail as yet. This despite its promising potential of this new "simplified triangle" technique. Such an investigation would be undoubted of key importance since it would inform on the potential usefulness of this technique when combined with one of the most sophisticated EO satellites currently in orbit.

In the purview of the above, the present study aims to explore, to our knowledge for the first time, the ability of the "simplified triangle" method used synergistically with Sentinel-3 data for predicting the spatiotemporal variability of both EF and SSM, at one experimental site located in Spain, belonging to the FLUXNET global in-situ monitoring network.

2. Materials

2.1 Study sites & In-situ data

Our experimental site consisted of the Albuera ("ES-Abr") experimental site located in Spain (38.702 Lat &-6.786 Lon, see **Figure 1**). The site is representative of a typical Mediterranean savannah ecosystem type and is a relatively flat area (279m asl). In the site it is installed a dense ground monitoring instrumentation network for the long term measurement of several parameters characterising land surface interactions. ES-Alb is part of the CarboEurope monitoring network, which part of FLUXNET, the largest global observational network today acquiring micro-meteorological fluxes and several ancillary parameters (Baldocchi et al., 1996).

In FLUXNET, all ground measurements are conducted using standardised instrumentation across the network sites.

In this study, ground measurements of the required parameters (i.e. LE, Rn, SSM at surface layer) were data collected from the ICOS (Integrated Carbon Observation System) database (http://www.europe-fluxdata.eu/icos/home) at Level 2 processing, to allow consistency and interoperability. Following the data acquisition, pre-processing that was applied to the data included the extraction of the specific days for which were available Sentinel-3 images at the experimental sites for that year, the computation of EF (as defined previously, i.e. LE/Rn). The final dataset of the in-situ measurements consisted of a total of 11 calendar days spanning the period from June to September 2018.

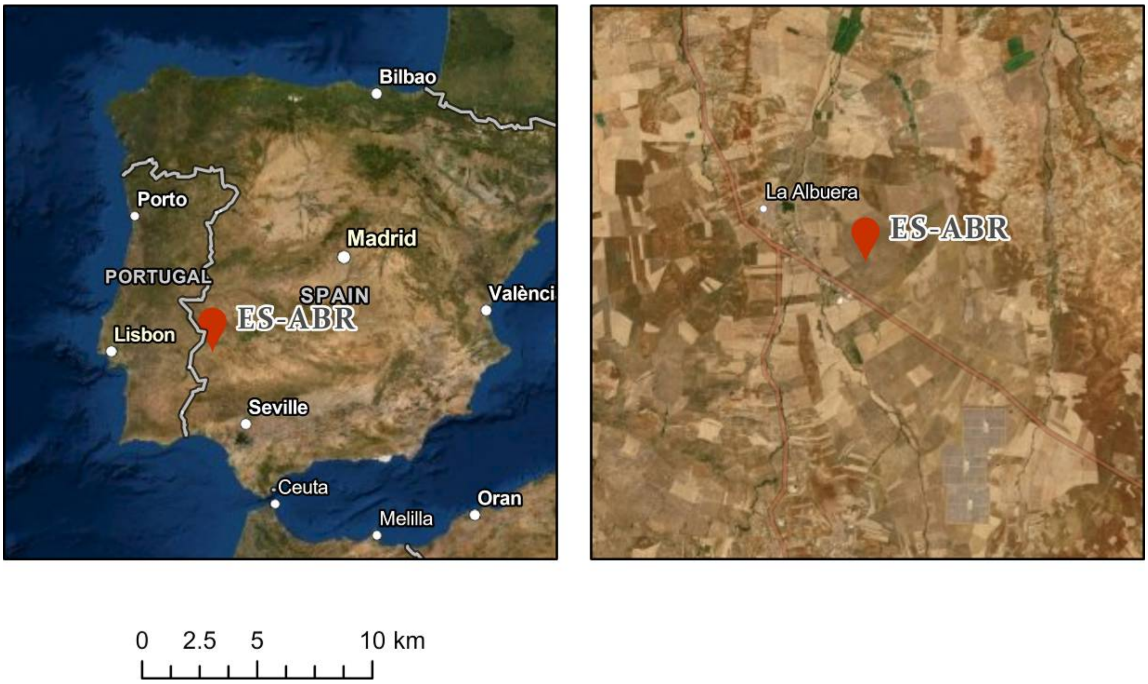

Figure 1: Study sites geographical location in Italy (left) & Spain (right) (background image source: ArcGIS Online)

2.2 Sentinel Data: Acquisition & Pre-Processing

Sentinel-3 is an EO satellite constellation developed by the European Space Agency (ESA) as part of the Copernicus Programme. It consists of 2 satellites, Sentinel-3A and Sentinel-3B. The Sentinel-3 satellites constellation allows a short revisit time of few than two days for the OLCI instrument and few than one day for SLSTR at the equator. The Sentinel-3 product used in this study included the Level 2 product named "SL_2_LST" (Birks, 2011). This product is the Land Surface Temperature (LST or Ts as defined previously) parameters provided to the users. The SL_2_LST product contains ten annotation files. The Fr is included among them. This Fr product was used in our study together with the LST/Ts (SLSTR ATBD Land surface Temperature, 2012). For the current study, this product was obtained for a total of 11 days of the year 2018, spanning from the start of the summertime period to the early autumn. The specific dates of the images used are the following ones: 23/06, 06/07, 09/07, 17/08, 25/08, 13/09, 20/09,21/09, 24/09, 5/09 and 28/09.To implement the method, first the Sentinel-3 images for the dates mentioned above were downloaded from CREODIAS (https://creodias.eu/). For each image, first a spatial subset was implemented covering the wider area of Spain only. Then, in each image product were retained only the layers of LST, Fr and NDVI. Then, each of those bands was masked for clouds and inland water using the masks already provided in each Sentinel-3 product. An example of which is illustrated in **Figure 2** below for a selected day.

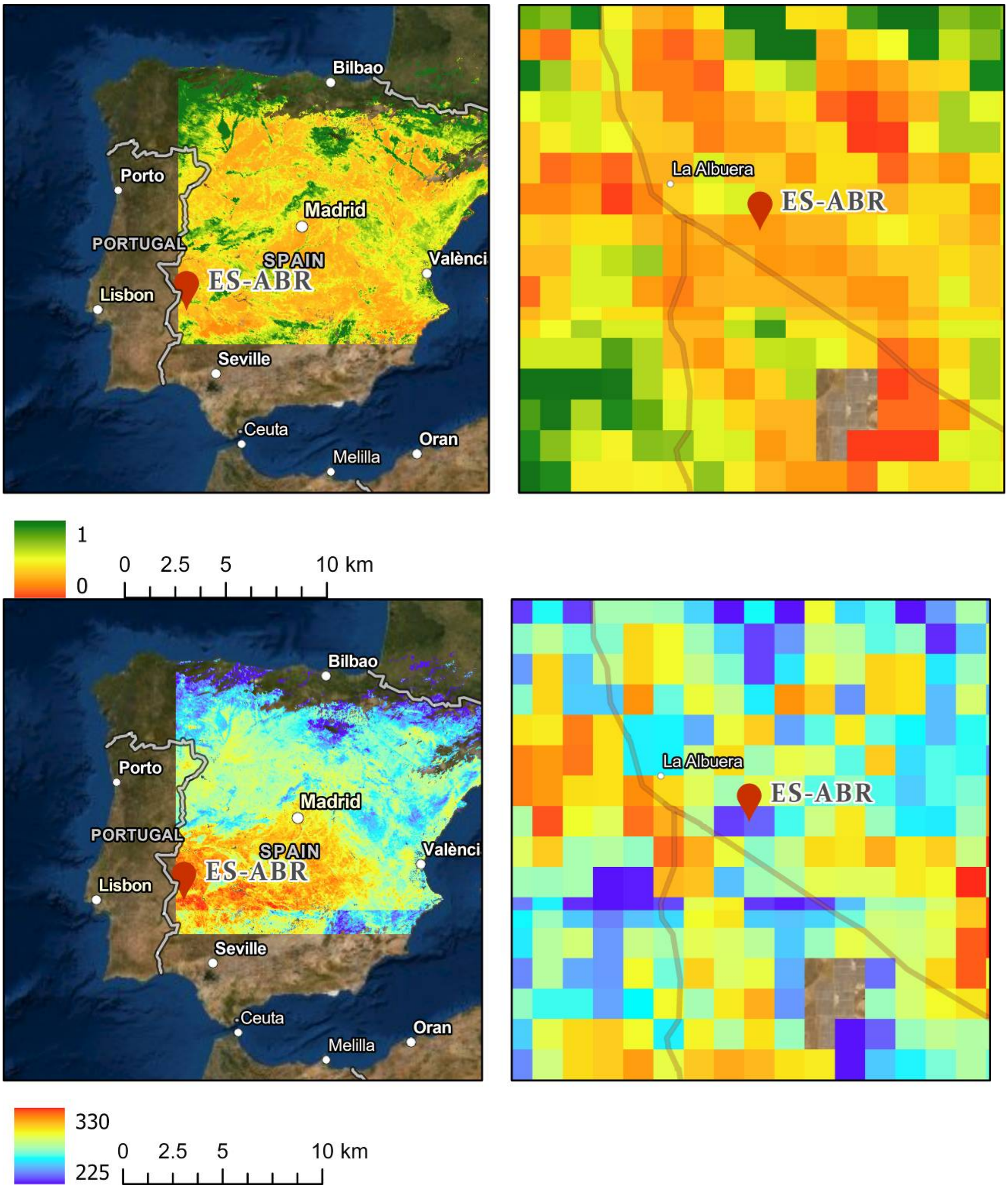

Figure 2: An example of final pre-processed Sentinel-3 images used as input in the "simplified triangle" implementation. The Fr map is shown on the top and the LST map on the bottom in each case. Sentinel-3 image acquisition is 25/08/2018.The geographical location of the study site is also indicated within the image.

3. Methods

Briefly, the method allows the estimation of two parameters, one being the surface wetness (Mo), and the other (EF) is defined as the ratio of evapotranspiration to net radiation (Rn). Mo applies only to the top few millimetres of the bare soil surface. Briefly, the method is based on constructing a scatterplot of radiometric surface temperature (Ts, or equally LST) versus the Fr. The basis of the method operation is illustrated in **Figure 3**.

The method requires an estimate of the Fr, which Carlson & Petropoulos (2019) propose can be derived from scaling the normalized difference vegetation index (NDVI). This required defining the NDVIo, NDVIs, which represent the NDVI values for bare soil and full vegetation cover respectively (see **Figure 3**) and then scaling NDVI using the formulae below (Gilles et al., 1997; Carlson, 2007):

$$\mathrm{Fr} = \left\{\frac{\mathrm{NDVI} - \mathrm{NDVI}_0}{\mathrm{NDVIs} - \mathrm{NDVI}_0}\right\}^2 \quad (1)$$

However, in Fr estimation, any other method can be equally used. Since the Fr layer was already provided in the Sentinel product, no further computation of Fr was performed.

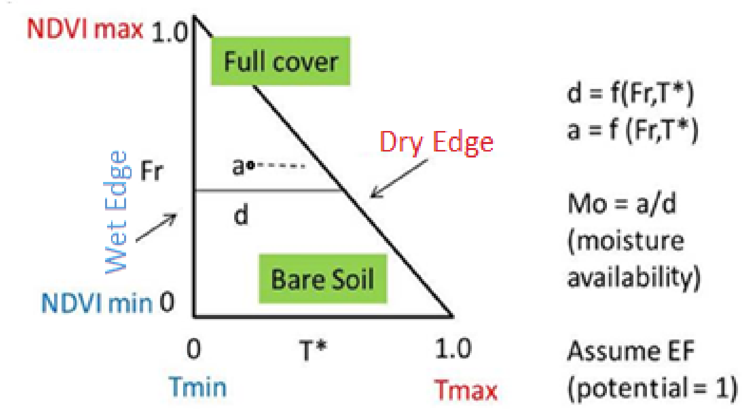

Figure 3: Simple geometry of the triangle. NDVI varies between its minimum and maximum values, respectively NDVIo and NDVIs, where NDVI is here scaled in Fr (after Carlson and Petropoulos, 2019).

NDVIs and Tmin, represent dense vegetation, define the lower left (wet or cold) vertex and the so-called 'wet edge' (or 'cold edge') of the triangle (refer to **Figure 3**). Similarly, NDVIo and Ts[max] define the lower right vertex of the triangle. The wet edge represents the limit of soil wetness and corresponds to the values of Mo and EF equal to 1.0. Another highly important feature, the 'dry edge' or 'warm edge' (also shown in **Figure 3**), represents the limit of soil dryness where Mo = 0 and extends from Ts [max] and NDVIo to NDVIs, which, for a triangle with a well-defined upper vertex, occurs at Ts[min]. Note that while Mo equals zero along the dry edge EF itself is non-zero along the dry edge except at the lower right vertex.

The next step in the method implementation involves the scaling of Ts to a variable named T*. To do this, the Ts for dry/bare soil needs to be determined, which is representative of the highest values of Ts for pixels found over dry/bare soil (Ts [max]) and the value of the minimum Ts representative of cool, wet pixels (Ts[min]) such as found over dense vegetation. Ts varies between its limits of Ts[min] and Ts[max]. The variable T* is scaled between 0 and 1 as defined below.

$$T^* = \{Ts - Ts\ (min)\} / \{(Ts\ (max) - Ts\ (min)\} \quad (2)$$

In our study, T^* was derived from the Fr/Ts scatterplot and by scaling the LST layer of each Sentinel-3 image (using Equation 1 above).

In the next step, Mo and EF are derived directly from Fr and T*. To do this, two important assumptions are made by the authors. The first is that transpiration (evaporation from the leaves) that always equals potential, at least when the vegetation is not at the wilting point. The second assumption is that the relation between EF and Mo varies linearly across the triangle domain. At bare soil fraction (equal to Mo), Mo is the availability of moisture on the surface, is the ratio between the lengths of a/d, both of these lengths being functions of the scaled radiometric surface temperature (T*) and Fr. Thus, Mo and EF are estimated as follows:

$$\mathrm{Mo} = 1 - \mathrm{T(pixel)/T(warm\ edge)} \quad (3)$$

$$\mathrm{EF} = \mathrm{EF_{soil}}(1 - \mathrm{Fr}) + \mathrm{Fr}\ \mathrm{EF}_{veg} = \mathrm{Mo}(1 - \mathrm{Fr}) + \mathrm{Fr} \quad (4)$$

Where EFsoil refers to the ratio of soil evaporation to net radiation.

The above mathematical expressions are valid on the assumption made by Carlson & Petropoulos (2019) that both Mo and EF vary linearly within the triangle between 0 and 1.0, such as (for Mo) between the cold and warm edges of the triangle. In addition, for each value of Fr and EF from the combined vegetation and bare soil, the canopy EF is assumed to be the weighted value of EF for the vegetation fraction of the pixel (EFveg = 1.0, by definition). In our study, the steps described above concerning the "simplified triangle" implementation were applied on each Sentinel-3 image, which resulted into obtaining two final image products for each image that was processed, namely the EF and Mo map. **Figure 4** shows an example of a scatterplots set that was created for one of the exprerimental days on which Sentinle -3 dayta had been acquired.

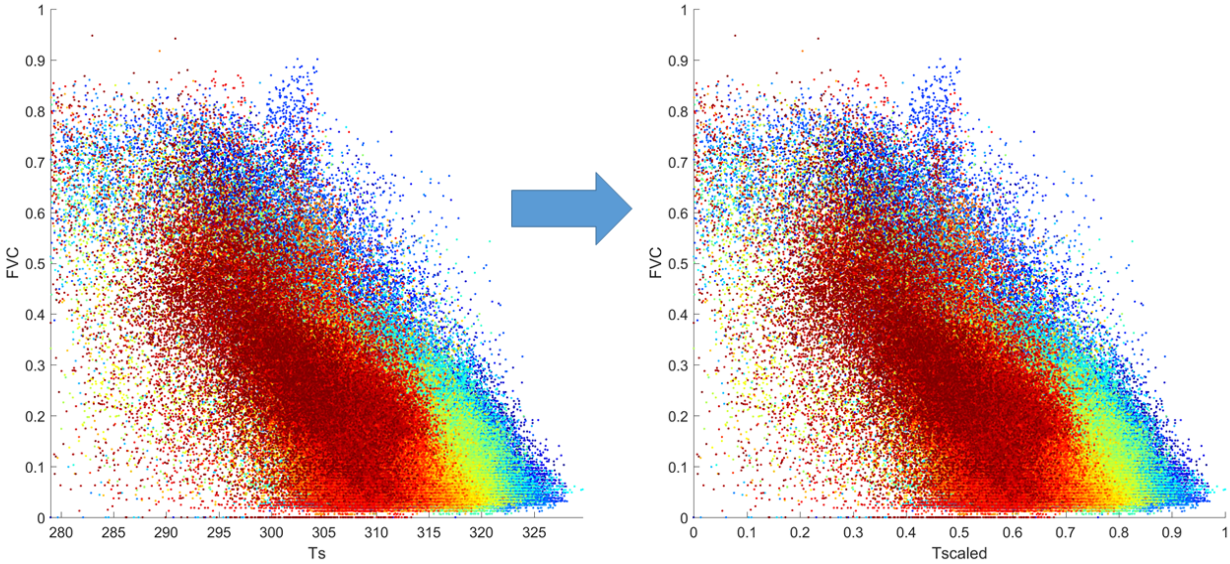

Figure 4: An example of the derived scatterplots during the technique implementation, shown here for the case of Sentinel-3 image with acquisition date of 25/08/2018. The use of color in the scatterplots is to support visualisation only.

3.2 Statistical Analysis

Point-by-point comparisons formed the main validation approach. In order to perform the SSM comparisons, in particular, Mo was converted to SSM using the soils' field capacity (an average value of which was used for each site). Similarly, in the in-situ data, the acquired volumetric moisture content (VMC, expressed as %) was converted to SSM. Also from the ground measurements, the EF was computed from the instantaneous latent heat fluxes (LE) and Rn. The statistical measures employed to quantify the agreement are summarised in **Table 1** below:

Table 1: Statistical measures used to assess the agreement between the predictions from the "simplified triangle" and the in-situ observations. Subscripts i = 1 … N denotes the individual observations', P denotes the predicted values, and O denotes the "observed" values. The horizontal bar denotes the mean value.

Name	Description	Mathematical Definition
Bias / MBE	Bias (accuracy) or Mean Bias Error	$bias = MBE = \frac{1}{N}\sum_{i=1}^{N}(P_i - O_i)$
Scatter / SD	Scatter (precision) or Standard Deviation	$scatter = \frac{1}{(N-1)}\sum_{i=1}^{N}\sqrt{(P_i - O_i - \overline{(P_i - O_i)})^2}$
MAE	Mean Absolute Error	$MAE = N^{-1}\sum_{i=1}^{N}\lvert P_i - O_i \rvert$
RMSD	Root Mean Square Difference	$RMSD = \sqrt{bias^2 + scatter^2}$
R	Pearson's Correlation Coefficient	$R = \frac{E\left[(\theta_{sat} - E[\theta_{sat}])(\theta_{in-situ} - E[\theta_{in-situ}])\right]}{\sigma_{sat}\sigma_{in-situ}}$

4. Preliminary results

An example of the EF and Mo maps obtained from the "simplified triangle" technique implementation for the Sentinel 3 image acquired on 25/08/2018 is illustrated in **Figure 5**. As can be observed, predicted EF and Mo exhibited mostly a spatially reasonable range and also a realistic variability spatially across the area covered in the satellite field of view. This spatial variability seems to also be in agreement to land use/cover of the area, the Fr and Ts maps (see for example **Figure 5** in combination with **Figure 2**) and the area topographical characteristics (i.e. slope, elevation). This observation, although it does not provide direct quantitative evidence of the EF product accuracy, suggests the examined method is able to provide reasonably the spatial variability in the EF and Mo.

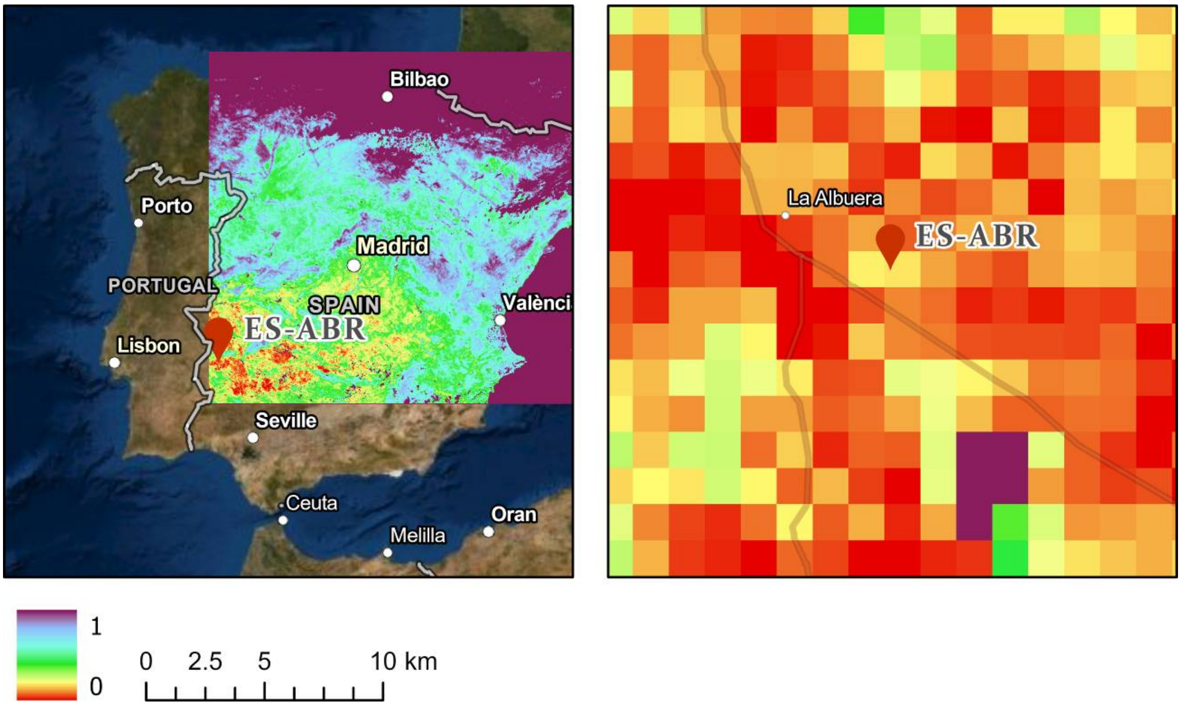

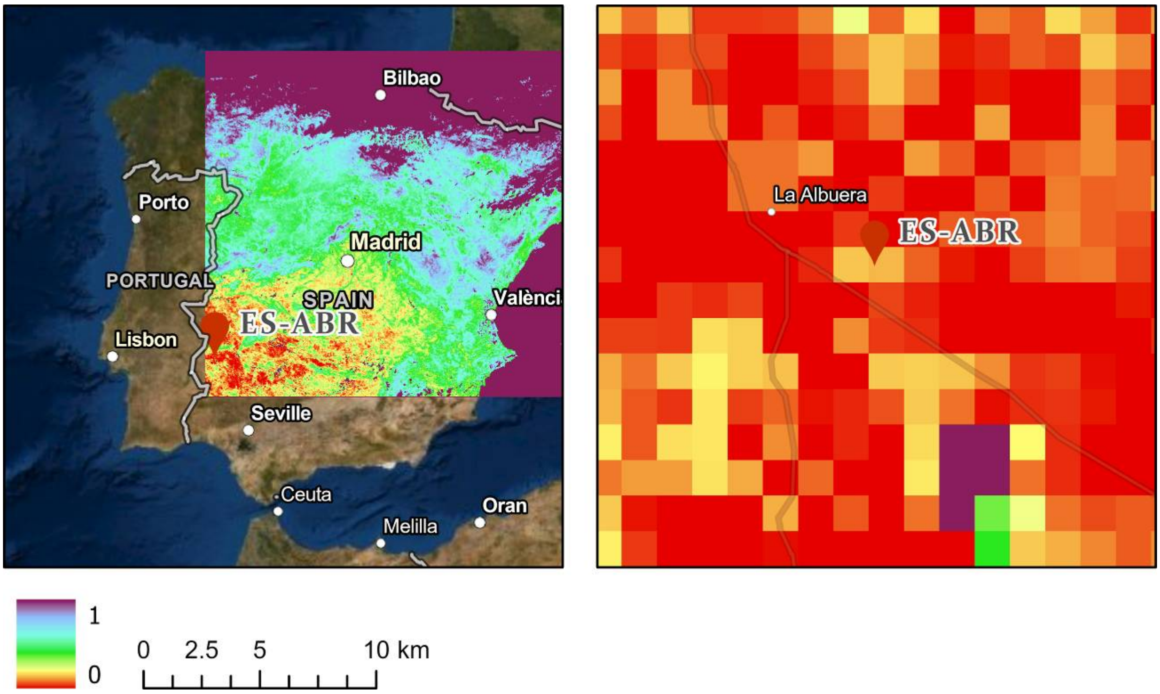

Figure 5: An example of a map of EF (top) and SSM (bottom) derived from the "simplified triangle" implementation using the Sentinel-3 data. Image acquisition date is 25/08/2018.

The main results from the quantitative comparisons obtained are summarised in **Table 2** and also in the scatterplot shown in **Figure 6,** which illustrated better the agreement found for the individual calendar days included in this study. As can be observed, EF has been predicted reasonably well in comparison to the reference data (i.e. ground observations), with a good R of 0.777, a RMSD of 0.063, a MBE of 0.028 and an SD of 0.057. As for the SSM comparisons, R was 0.439 (lower in comparison to the EF comparisons), whereas the RMSD was 0.048 vol vol^{-1}, well below the 0.1 vol vol^{-1} operational limit. MBE and SD were -0.04 and 0.027 vol vol^{-1} respectively. All in all, quantitative comparisons showed that the "simplified triangle" was able to provide predictions of both EF and SSM that were in good agreement to the collocated ground observations, which consisted the reference data. In terms of RMSD, prediction accuracy was better for EF in comparison to SSM, with the predicted EF slightly overestimated, whereas the predicted SSM was slightly underestimated. Because of the small number of tested days (11 in total), we cannot confirm that the MBE presented has statistical significance. It can be observed that the correlation between predictions and observations was significantly better for EF than the SSM comparisons.

Table 2: Summary of the statistical agreement for both EF and SSM for all days

	Bias / MBE	Scatter / SD	MAE	RMSD	R
EF	0.028	0.057	0.055	0.063	0.777
SSM	-0.040	0.027	0.04	0.048	0.439

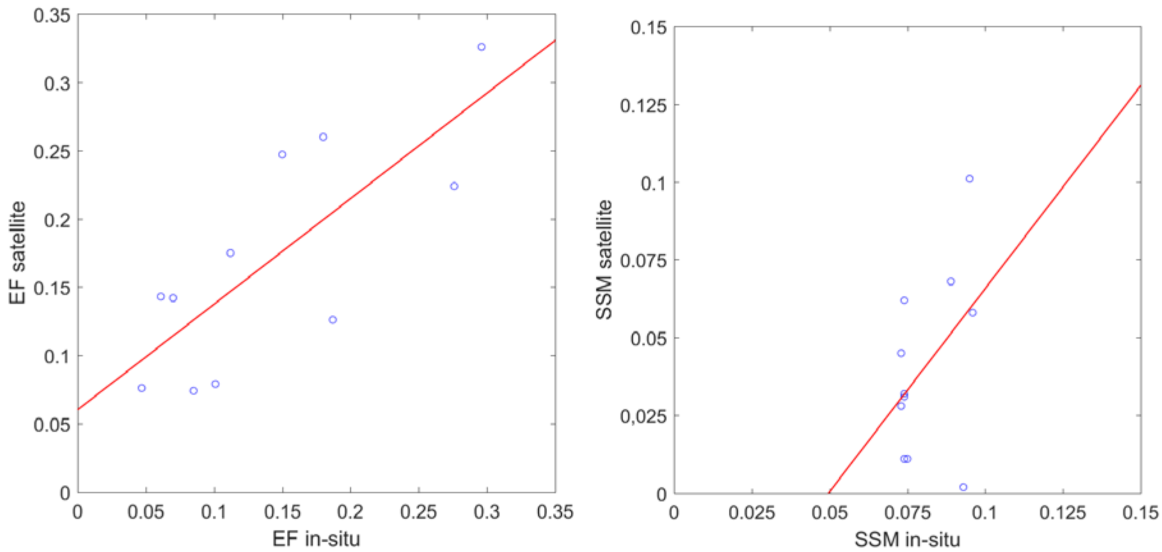

Figure 6: Comparisons for all days on which the technique was implemented between the in-situ measurements and satellite product values, for both EF (left) and SSM (right). Red lines represent the trend lines.

As can be seen in Figure 6, the trend line for the EF scatterplot shows a good fit, exhibiting p-value of 0.005. However for the SSM scatterplot trend line has a problematic p-value of 0.177. This caused by the small range of SSM in situ values that range from 0.073 to 0.096 vol vol^{-1} while the SSM predicted by Sentinel-3 presents a higher range, with values between 0.002 and 0.101 vol vol^{-1}. This disparity in the range also affects the correlation coefficient and is reflected in the relatively high bias (-0.04 vol vol^{-1} while the RMSD is 0.048).

5. Discussion

The investigation performed in this work, the first application of the "simplified triangle technique" on Sentinel-3 EO data, resulted in promising results in deriving spatiotemporal estimates of both SSM and EF. The results support that the simplified triangle technique can provide reasonably accurate predictions of both parameters. Several studies (i.e. Chan et al., 2016, Bindlish et al., 2015) have already made a strong case for the utility of the in situ SSM estimates in order to correctly assess the accuracy of satellite SSM products.

In regards to EF, it is noted that higher estimation accuracy was achieved for the LE/Rn and H/Rn fluxes compared with other methods that use a slightly different estimation method for EF (Peng and Loew, 2014; Lu et al., 2015). However, direct comparisons of results results obtained herein against results where EF has been estimated using different approaches is not a feasible practice and could lead to erroneous conclusions. Prediction accuracy of SSM with the "simplified triangle" was close or even improved compared to studies that use different Ts/VI methods (e.g. Carlson and Capehart, 1997; Gillies et al. 1997).

There are various explanations for the imperfect agreement in the case of the EF comparisons, despite the estimated EF having strong correlation and low RMSD with the measured EF.

Cloud cover has been identified as a critical factor influencing the stability of EF predictions during daytime (Hall et al., 1992). Despite the images being collected from May to September, cloudiness could have affected the radiation received by the validation site. Instrumentation accuracy could have also negatively impacted the agreement between the estimated and measured EF. Generally, the instrumental uncertainty regarding measurement of Rn is of the order of ◎10%, tho angle/measurement volume (particularly in cases of sloped terrain). Also typical uncertainty in the estimation of Tair is ~ 2 ºC. Uncertainty in the estimation of the turbulent fluxes by the eddy covariance system is typically in the order of 10-15 % (e.g. Petropoulos et al., 2015), and according to some researchers potentially more when the eddy covariance system is installed in non-flat terrain (e.g. Schmid and Lloyd, 1999). As of the SSM comparisons, the mismatch of the horizontal and vertical coordinates between the location of the station and the satellite pixel was shown to negatively affect correlation. Furthermore, the prediction from the satellite is responding to the soil water content in the top few milimeters of the soil, a much shallower layer than the ground measurements (Petropoulos et al., 2018; Deng et al., 2019).

Another potential factor in both the EF and SSM retrievals could be related to the method that the Fr was computed. The present study utilized the Fr that was provided directly from Sentinel-3. This Fr is computed using a different approach than the NDVI scaling suggested by Carlson & Petropoulos (2019). To our knowledge, the sensitivity of the "simplified triangle" to the Fr and Ts computation method has not yet been sufficiently investigated to allow a quantification of the influence of the specific Fr method selected in this study. However, results of a preliminary investigation (results not shown in this study) indicate that the estimation method of Fr is affecting the predictions of EF and SSM significantly. For illustration purposes only, **Figure 6** presents the difference in the scatterplots between the two Fr estimation methods. On the right, there is the scatterplot using the sentinel-derived Fr. On the middle is the Fr derived from NDVI scaling technique (Carlson & Petropoulos, 2019). The significant differences of the derived Fr consequently may have an important bearing to the "simplified triangle" technique implementation. This is an area requiring further investigation.

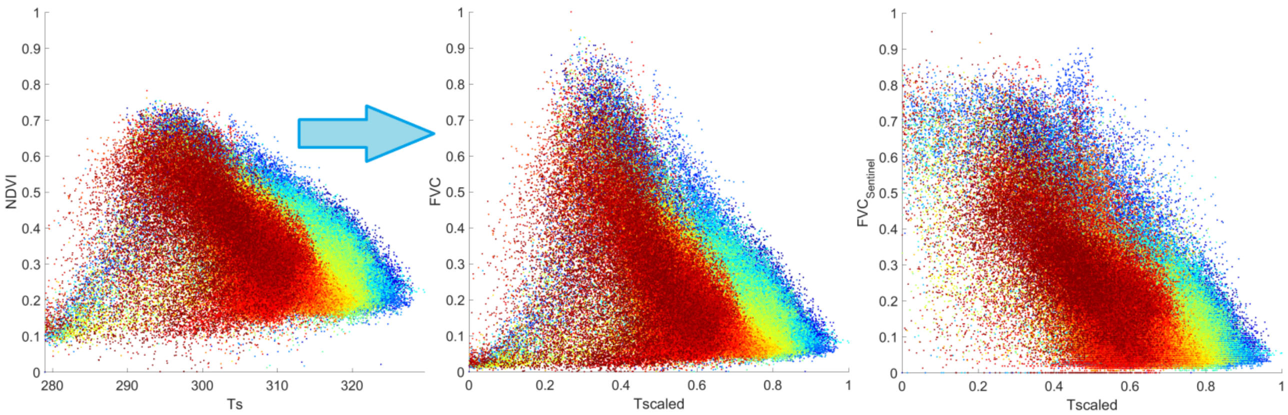

Figure 6: An example of scatterplot created initially on the ordinate the NDVI (left), the Fr computed from the NDVI scaling (middle) and the Fr from the Sentinel product. All image

layers refer to the Sentinel-3 image with acquisition date is 25/08/2018. The use of color in the scatterplots is to support visualisation only.

Finally, the spatial resolution differences between the CarboEurope point measurements (5 m x 5 m) and Sentinel-3 pixel resolution (1 km x 1 km) increase the degree of uncertainty of the validation for both EF and SSM (Stisen et al., 2008). In situ measurements cannot represent SSM or EF at the same spatial scale within the large footprint of the Sentinel-3 product. Thus, the averaged value of SSM is often represented as reference value. Several studies (Wagner et. al., 2013, Petropoulos et al., 2015b) have shown that point based measurements cannot sufficiently represent the absolute value of SSM for large pixels. Such representation can be achieved by upscaling the point estimates using techniques like those proposed by Srivastava, (2017). Dense in situ networks are very useful in this regard if present at the location of interest.

6. Conclusions

In this study, the ability of the so-called “simplified triangle” technique was evaluated when used with Sentinel-3 EO data. The ability of the method to predict EF and SSM was evaluated for 11 days of the year 2018 at an experimental site in Spain belonging to the CarboEurope operational network. To our knowledge, this study represents the first attempt to examine this specific technique’s accuracy using Sentinel-3 data in a typical Mediterranean savannah ecosystem.

A satisfactory agreement for both EF and EF an RMSD was reported, with Root Mean Square Error (RMSE) of 0.063 and 0.048 vol vol^{-1} and a correlation coefficient (R) of 0.777 and 0.439 for EF and SSM respectively. This prediction accuracy is comparable to that reported in other similar studies where the same technique has been implemented with dissimilar EO data. The RMSD for the SSM was below the 0.1 vol vol^{-1} limit. Evidently, the “simplified method” allows one to make estimates of EF and SSM and over an area using just a few simple calculations in conjunction with satellite or aircraft images made at optical wavelengths and thermal infrared. The technique seems to have a significant advantage over other methods belonging to this same group of models in that it requires no land surface model or an ancillary surface or atmospheric data for its execution and is easy to apply. Yet, more work is required to evaluate its predictions in a wide range of ecosystem, and environmental conditions globally and the sensitivity of the Fr and Ts to the EF and Mo predicted by the technique. All in all, the results of this study are of considerable scientific and practical value in regards to the evaluation of the potential of the examined technique for deriving key biophysical parameters of the Earth’s system.

Acknowledgements

In the present work, the participation of Dr Petropoulos has received funding from the European Union’s Horizon 2020 research and innovation programme ENViSIoN-EO under the

Marie Skłodowska-Curie grant agreement No 752094. Special thanks to Dr. Andrew Pavlides for his assistance with Figures 4 and 6. Authors are also grateful to the anonymous reviewers for their comments that helped to improve the manuscript.

References

1. Amri, R., Zribi, M., Lili-Chabaane, Z., Szczypta, C., Calvet, J. C., Boulet, G. (2014) FAO-56 Dual Model Combined with Multi-Sensor Remote Sensing for Regional Evapotranspiration Estimations, *Remote Sensing*, 6, (5387-5406)
2. Baldocchi, D., Valentini, R., Oechel, W. and R. Dahlman (1996) : Strategies for measuring and modelling carbon dioxide and water vapor fluxes over terrestrial ecosystems. *Global Change Biol*. 2, 159–168.
3. Birks, Andrew; Cox (14 January 2011). "SLSTR: Algorithm Theoretical Basis Definition Document for Level 1 Observables" (PDF). Science & Technology Facilities Council Rutherford Appleton Laboratory: 173.
4. Carlson TN (2007). An overview of the “triangle method” for estimating surface evapotranspiration and soil moisture from satellite imagery. *Sensors* 7:1612-1629
5. Carlson, T.N. & G.P. Petropoulos (2019): A New Method for Estimating of Evapotranspiration and Surface Soil Moisture from Optical and Thermal Infrared Measurements: The Simplified Triangle. *International Journal of Remote Sensing*, 40(20), 7716-7729, DOI: 10.1080/01431161.2019.1601288.
6. Carlson, T.N., Capehart, W.J., and R. R., Gilies (1995): A new look at the simplified method for remote sensing of daily evapotranspiration, Rem. Sens. Envir. 54: 161-167
7. Chan, S. K., R. Bindlish, P. E. O'Neill, E. Njoku, T. Jackson, A. Colliander, *et al.*, "Assessment of the SMAP passive soil moisture product," *IEEE Transactions on Geoscience and Remote Sensing,* vol. 54, pp. 4994-5007, 2016.
8. Coudert, B., Ottlé, C., &Briottet, X. (2008) Monitoring land surface processes with thermal infrared data: Calibration of SVAT parameters based on the optimisation of diurnal surface temperature cycling features, *Remote Sensing of Environment*. 112 3 [872-887]
9. Deng, K.A.K.; Lamine, S.; Pavlides, A.; Petropoulos, G.P.; Srivastava, P.K.; Bao, Y.; Hristopulos, D.; Anagnostopoulos, V. Operational Soil Moisture from ASCAT in Support of Water Resources Management. *Remote Sens.* **2019**, *11*, 579.
10. European Commission (2009) White Paper, Adapting to climate change: Towards a European framework for action. COM (2009), 147 (4).
11. Gillies, R. R., Carlson, T. N., Cui, J., Kustas, W. P., Humes, K. S. (1997). Verification of the “triangle” method for obtaining surface soil water content and energy fluxes from remote measurements of the Normalized Difference Vegetation Index NDVI and surface radiant temperature. *International Journal of Remote Sensing*, 18, 3145–3166.

12. Hall, F.G., Huemmrich, K.F., Goetz, S.J., Sellers, P.J., and J.E., Nickeson, (1992). Satellite remote sensing of the surface energy balance: success, failures and unresolved issues in FIFE. *J. Geophys*. Res. 97 (D17), 19061–19089.
13. IPCC (2009) Summary report of the IPCC expert meeting on the science of alternative metrics 18–20 March 2009, Oslo, Norway. IPCC-XXX/Doc.13 (31.III.2009) Available at www.ipcc.ch/meetings/session30/doc13.pdf
14. Lu, J., Tang, R., Shao, K., Li, Z. L., Zhou, G. (2015). Assessment of two temporal-information-based methods for estimating evaporative fraction over the Southern Great Plains. *International Journal of Remote Sensing*, 1-17.
15. Maltese, A., Capodici, F., Ciraolo, G., Loggia, G. L. (2015). Soil Water Content Assessment: Critical Issues Concerning the Operational Application of the Triangle Method. Sensors 15(3), 6699-6718.
16. Peng, J., Loew, A. (2014). Evaluation of Daytime Evaporative Fraction from MODIS TOA Radiances Using FLUXNET Observations. *Remote Sensing*, 6(7), 5959-5975.
17. Petropoulos, G. P., Carlson, T. N., Wooster, M. J., Islam, S. (2009). A Review of Ts/VI Remote Sensing Based Methods for the Retrieval of Land Surface Fluxes and Soil Surface Moisture Content. *Advances in Physical Geography* 33(2):1-27.
18. Petropoulos, G. P., G. Ireland, and P. K. Srivastava, "Evaluation of the soil moisture operational estimates from SMOS in Europe: results over diverse ecosystems," *IEEE Sensors Journal*, vol. 15, pp. 5243-5251, 2015.
19. Petropoulos, G.P., G. Ireland, S. Lamine, N. Ghilain, V. Anagnostopoulos, M.R. North, P.K. Srivastava & H. Georgopoulou (2016): Evapotranspiration Estimates from SEVIRI to Support Sustainable Water Management. *Journal of Applied Earth Observation & Geoinformation*, 49, 175-187, DOI 10.1016/j.jag.2016.02.006.
20. Petropoulos, G.P., Ireland, G. & B. Barrett (2015): Surface Soil Moisture Retrievals from Remote Sensing: Evolution, Current Status, Products & Future Trends. *Physics and Chemistry of the Earth*. DOI: 10.1016/j.pce.2015.02.009.
21. Petropoulos, G.P., P.K. Srivastava, K.P. Feredinos & D. Hristopoulos (2018): Evaluating the capabilities of optical/TIR imagine sensing systems for quantifying soil water content. *Geocarto International*, DOI 10.1080/10106049.2018.1520926.
22. Piles, M., G.P. Petropoulos, N. Sanchez, A. González-Zamora & G. Ireland (2016): Towards Improved Spatio-Temporal Resolution Soil Moisture Retrievals From the Synergy of SMOS & MSG SEVIRI Spaceborne Observations. *Remote Sensing of Environment*, 180, pp:403-471, DOI 10.1016/j.rse.2016.02.048.
23. R. Bindlish, T. Jackson, M. Cosh, T. Zhao, and P. O'Neill, "Global soil moisture from the Aquarius/SAC-D satellite: Description and initial assessment," *IEEE Geoscience and Remote Sensing Letters*, vol. 12, pp. 923-927, 2015.
24. Schmid, H. P. and C. R., Loyd (1999): Spatial representativness and the location bias of flux footprints over inhomogeneous areas. *Agric. And Forest Meteor*., 93, 195-209.

25. Silva-Fuzzo, D., T.N. Carlson, N. Kourgialas & G.P. Petropoulos (2020): Coupling Remote Sensing with a water balance model for soybean yield predictions over large areas. *Earth Science Informatics*, [in press].
26. SLSTR ATBD Land Surface temperature (2012): Sentinel-3 Optical Products & Algorithm Definition. Version 2.3, Available from https://sentinel.esa.int/web/sentinel/technical-guides/sentinel-3-slstr/level-2/calculate-vegetation-fraction [Accessed on 10/04/2020].
27. Srivastava, P.K., "Satellite soil moisture: Review of theory and applications in water resources," *Water Resources Management,* vol. 31, pp. 3161-3176, 2017.
28. Srivastava, P.K., P. C. Pandey, G.P. Petropoulos, N. K. Kourgialas, S. Pandley & U. Singh (2019): GIS and remote sensing aided information for soil moisture estimation: A comparative study of interpolation technique. *Resources* MDPI, 8(2), 70.
29. Steinhaeuser, K., Ganguly, A. R., & Chawla, N. V. (2012) Multivariate and multiscale dependence in the global climate system revealed through complex networks, *Climate dynamics*. 39 (889-8950
30. Stoyanova, J. S., & Georgiev, C. G. (2013). SVAT modelling in support to flood risk assessment in Bulgaria. *Atmospheric Research*, 123, 384-399
31. Wagner, W., S. Hahn, R. Kidd, T. Melzer, Z. Bartalis, S. Hasenauer, *et al.*, "The ASCAT soil moisture product: A review of its specifications, validation results, and emerging applications," *Meteorologische Zeitschrift,* vol. 22, pp. 5-33, 2013.